scientific reports

Check for updates

OPEN

Spatial-temporal modeling of urban resilience and risk to earthquakes

Fatema Rahimi[1,3], Abolghasem Sadeghi-Niaraki[1,3], Mostafa Ghodousi[2] & Soo-Mi Choi[1]✉

In the face of burgeoning urbanization, cities and residential areas are increasingly vulnerable to diverse hazards. This research develops a spatial-temporal assessment of Bojnord City's earthquake risk and resilience, concentrating on the morning, evening, and nighttime periods. After a thorough assessment of the literature, the research identified seven key criteria and 27 sub-criteria that address important aspects. Fuzzy logic was utilized for data standardization and the DANP approach was employed to weight the criteria in order to appropriately assess resilience and risk. The IO and OWA models were used to integrate these criteria, and the results showed notable spatial and temporal disparities in risk and resilience. The results highlight the significance of integrating both temporal and spatial aspects in risk assessments and urban resilience evaluations to enhance the effectiveness of disaster management plans. The findings demonstrate that some regions are always at high risk and low resilience, regardless of the time of day, emphasizing the necessity of focused, continuous disaster preparedness plans. This approach not only validates the consideration of the dynamic criteria but also provides a replicable methodology for other cities facing similar seismic threats.

Keywords Resilient, Spatial-temporal resilience, Earthquake, DANP method

Today, cities and residential areas are built in places that are exposed to natural and human-made disasters due to natural hazards[1]. Humans have faced earthquakes as a natural hazard throughout history and suffered tremendous social and economic losses[2]. Until the 1980s, the dominant perspective in disaster and urban management was more confrontational and aimed to reduce the level of vulnerability. Therefore, in recent years, significant changes have been seen in the attitude toward risks at the global level, as the dominant view has shifted to increasing resilience against disasters[3]. The fact is that it is not possible to predict future risks based on evidence, and it is therefore necessary to assess the resilience of the local community to prevent an increase in vulnerabilities[4]. Resilience is a form of foresight due to the dynamic nature of society's response to risks. Considering the variety of applications of resilience, practical and theoretical understanding of this concept requires evaluation, measurement, and modeling.

Therefore, in this research, a spatial information system (GIS) is used to analyze spatial indicators of resilience because most urban resilience indicators have a spatial nature. The importance of risk assessment in this context also cannot be overstated. Risk assessment, which considers the vulnerabilities and risks of a particular location, is an essential tool for comprehending the potential impacts of earthquakes. From a scientific perspective, risk assessment offers a framework to quantify and model the interactions between these factors, giving researchers a clearer picture of the potential locations and types of earthquake damage. This process is essential for identifying areas most vulnerable to earthquakes, enabling targeted interventions to enhance safety and resilience.

From the 1980s onwards, especially in the 1990s, social science researchers believed that vulnerability had a social character and was not limited to demographic and physical damage. Factors such as population, population density, demographic characteristics, etc., are key social indicators for assessing resilience. The issue raised in the assessment of resilience is that some resilience criteria change over time, including population density. Population density is a criterion used to measure population load in resilience[2]. Due to the different conditions of human activities, their distribution in different places is heterogeneous and dependent on time[5]. Identification and analysis of human movement behavior can lead to the extraction of movement patterns on an urban scale[6]. In the case of hazardous events, it is very important to have information about population distribution with the highest possible spatial and temporal quality for effective resilience assessment and earthquake risk. These

[1]Department of Computer Science and Engineering and Convergence Engineering for Intelligent Drone, XR Research Center, Sejong University, Seoul, Korea. [2]Geoinformation Technology Center of Excellence, Faculty of Geodesy & Geomatics Engineering, K.N. Toosi University of Technology, 19697 Tehran, Iran. [3]Fatema Rahimi and Abolghasem Sadeghi-Niaraki contributed equally to this work. ✉email: smchoi@sejong.ac.kr

concepts and the importance of paying attention to urban resilience clearly explain the necessity of evaluating and spatial-temporal modeling of urban resilience against earthquakes and risk assessment. This research aims to address the spatial-temporal modeling of urban resilience against earthquakes and earthquake risk through the publicly available data and spatial-temporal distribution of the population, using an objective approach and spatial information systems. The contributions of this research are fourfold as follows:

1. Resilience modeling with an objective (quantitative) approach and publicly available data.
2. Consideration of the spatial-temporal dimension of population density as a criterion.
3. Spatial-temporal modeling of urban resilience against earthquakes and earthquake risk assessment considering physical and social dimensions.

This study identifies and employs seven key criteria, each of which is further broken down into 27 sub-criteria, to comprehensively assess urban resilience and risk. The seven key criteria include accessibility to vital centers, hazard assessment, distance from the human danger zone, traffic factors (property of communication network), substrate characteristics, distance from geological factors, physical characteristics of the building, and demographic composition. The selection of these criteria was informed by a rigorous process that included literature reviews, expert consultations, and the availability of data specific to the study area. Table 1 provides an overview of the criteria and sub-criteria used in this study.

Significantly, in most of the study areas, resilience is low and risk is high, particularly in areas with heightened levels of hazard and vulnerability, while response capacity is low. Conversely, lower-risk regions exhibit decreased vulnerability and potential hazards. The results of the study show that there are notable spatial and temporal differences in risk and resilience in Bojnord City. It is noteworthy that certain areas constantly show low resilience and high risk, regardless of the time of day, underscoring the necessity of ongoing, 24/7 disaster planning. The importance of including both temporal and spatial elements in risk assessments and urban resilience is highlighted by these findings.

The article progresses as follows: Sect "Literature review" presents a comprehensive review of prior research. Sect "Study area and dataset" introduces the study area, providing crucial context for the research. Sect "Methodology" outlines the methodology employed for both resilience and risk assessment, detailing the analytical framework and techniques used. The subsequent Sects "Results" and "Discussion" cover the results and discussions, offering insights derived from the research. Finally, Sect "Conclusion and future work" encapsulates the conclusion and outlines potential avenues for future work, inviting engagement from other researchers.

Literature review

One of the most important issues in cities is the resilience of urban areas against risks and disasters[7]. Therefore, this topic has been of interest to researchers for quite some time, and so far, several studies have been conducted in this field, which we will discuss. Cutter, Ash[8] evaluated and spatially modeled the resilience of a region in the United States according to indicators of social, economic, community, environmental, organizational, and infrastructure dimensions. Statistical data were used in the mentioned research (objective approach). After collecting the data and normalizing them, the consistency of the indicators was measured using Cronbach's alpha test. The value of Cronbach's alpha was 0.67, which indicates a significant relationship between indicators and urban resilience. Joerin, Shaw[9] assessed resilience against climate change in India. There, the assessment of resilience against climate change was determined by the weighted average method. The results showed that there was a correlation between the indicators and dimensions of resilience. Parizi, Taleai[10] determined urban resilience according to the indicators of the physical dimension and the relationships between them. In that study, the DEMATEL method was used to analyze and determine the quantitative relationships of the indicators, and the results showed that physical resilience indicators can be used in urban planning. Zhao, Yang[11] evaluated urban resilience against earthquakes according to 20 indicators from the physical dimension. They aimed to investigate the relationships between urban resilience indicators using the fuzzy total interpretive structural model (FTISM). Similarly, Liu, Lei[12] reviewed and analyzed the resilience of 30 provincial capital cities in China from 1998 to 2017. Based on those results, they proposed measures for the development of urban resilience. Zhai, Zhao[13] evaluated seismic resilience for the urban environment by combining three indicators of secondary disaster risk, engineering, and non-engineering systems.

However, the problem remains that few studies have assessed resilience through a comprehensive approach. Another issue is the spatial nature of resilience indicators, which has received little attention. Resilience assessment has both objective (quantitative) and subjective (qualitative) approaches[2]. Most of the studies on resilience have been conducted using the subjective approach, and the objective approach has received less attention. One of the advantages of evaluating resilience with an objective approach is the use of publicly available data (secondary

Dataset	Source	Year	Data description
Land use	Municipal Information and Communication Technology Organization	2004	Categories such as residential, commercial, educational, healthcare, hospitality, transportation, and traffic networks
Gas pipeline	North Khorasan Gas Transmission Company	2015	Pipeline attributes including material type, pressure levels, diameter, and length
Population	Statistics Center of Iran	2016	Data on population size and age group distributions by neighborhood and district
Taxi origion-destination	Hamsi application (SACO Company)	2018	Details of taxi trips including ID, GPS coordinates, speed, time, direction, and passenger status

Table 1. Overview of primary datasets.

data). Resilience assessment becomes effective when it is quantifiable, objective, and based on spatial analysis. Also, in most studies conducted to evaluate and measure urban resilience, the spatial-temporal component and behavioral patterns of the population have been overlooked. Therefore, it is necessary to incorporate the time dimension to measure resilience.

Alongside the evaluation of resilience, risk assessment has been an important area of research, especially when it comes to earthquakes. Various models and approaches have been established in recent studies to evaluate and prioritize risks in urban areas to minimize potential damage and casualties. By incorporating hazard, vulnerability, and response capacity into comprehensive models, these studies have advanced the assessment of earthquake risk. Mili, Hosseini[14] introduced the "Integrated Earthquake Safety Index" (IESI) to evaluate urban safety levels, applying it in Tehran to prioritize risk reduction measures. This holistic approach is closely aligned with urban resilience principles, considering both physical and socio-economic factors. Kamranzad, Memarian[15] assessed earthquake risk in Tehran using GIS-based datasets, creating detailed hazard and vulnerability maps through a combination of probabilistic and deterministic methods. This GIS-based approach allows for precise spatial analysis, making it easier to identify high-risk zones and prioritize interventions. Jena, Pradhan[16] reviewed seismic hazard and risk models, emphasizing GIS-based approaches and the potential of machine learning to enhance risk assessment. The use of GIS in these models makes it possible to integrate various information, providing a more dynamic and in-depth understanding of risk across various metropolitan regions. Aydın, Birincioğlu[17] used the Analytical Hierarchy Process (AHP), integrating quantitative data and expert opinion to evaluate earthquake risk. The multi-criteria method used in the study emphasizes the significance of assessing a variety of risk factors to ensure a more comprehensive and reliable risk assessment. This study's continuous application of GIS-based methods emphasizes their importance for assessing earthquake risk. GIS makes it easier to integrate and visualize complicated data, which enables more accurate and context-specific risk evaluations. Including the spatial-temporal aspect of risk in our analysis is a significant improvement since it acknowledges that risk is not constant but varies over time due to changes in population density and other factors. Through the integration of spatial analysis and these temporal dynamics, our approach aligns risk assessment closer to resilience strategies. This integration ensures that the changing nature of urban surroundings is considered when evaluating risk and resilience. This allows for more effective planning and response methods that are sensitive to the location and timing of future seismic events.

Study area and dataset

Study area

Bojnord, the capital city of North Khorasan Province in northeastern Iran, is selected for this study due to its significant seismic risk and urban development challenges. Bojnord is an approximately 36-square-kilometer area at latitude 37°28' and longitude 57°20'. It is situated at the foothills of the Aladagh, Koppeh Dagh, and Alborz mountain ranges. This geographical location contributes to its high susceptibility to seismic activity.

One of Iran's seismically active areas is the province of North Khorasan. Within 300 km of North Khorasan, 152 earthquakes with magnitudes of 4 or higher have been reported over the past ten years, or about one every month on average. On average, there is one earthquake near North Khorasan every 24 days, indicating a fairly high frequency of seismic events. In 2021 alone, 25 earthquakes with magnitudes of 4 or greater were reported within this radius, with the most powerful having a magnitude of 5.4. Figure 1 provides historical context for the seismic risk of the city by providing detailed information on previous earthquakes that have affected Bojnord and the surrounding area[18].

The city's rapid development and influx of migrants, along with these regular seismic events, have increased Bojnord's vulnerability. The city's rapid industrial and urban growth during its development has led to

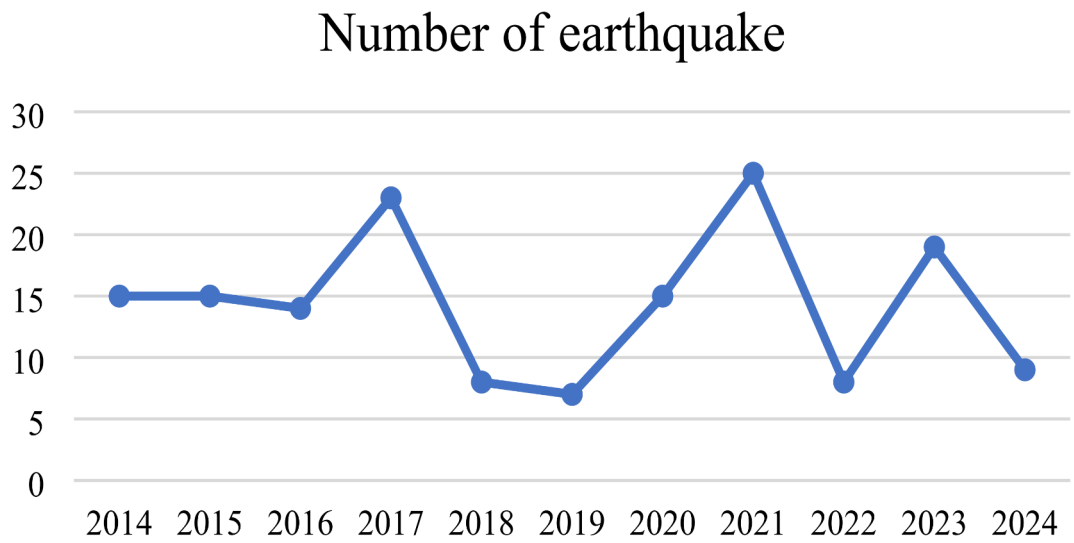

Fig. 1. Annual earthquakes with a magnitude of 4 or higher within 300 km of Bojnord[18].

infrastructure that often does not align with the changing needs of its population, which raises the seismic risk. Furthermore, North Khorasan has experienced plenty of other natural disasters, such as landslides, floods, and frost, all of which have caused significant damage to structures and infrastructure. This emphasizes how crucial it is to assess Bojnord's resilience to earthquakes. The study area's location and important locational details are shown in Fig. 2.

Dataset

This study utilizes multiple datasets to evaluate urban resilience and disaster risk. Table 1 provides an overview of the primary datasets employed in the analysis, including their sources, years of collection, data types, and descriptions. These datasets encompass information on land use, population, gas pipelines, and taxi origin-destination data, which together form a comprehensive basis for assessing urban dynamics and resilience.

Land use data

Land use data were acquired from the Municipal Information and Communication Technology Organization. This dataset includes vector polygons representing various land use categories such as residential zones, workplaces, educational institutions, kindergartens, healthcare facilities (clinics and hospitals), tourist accommodations, restaurants, road networks, and traffic monitoring stations.

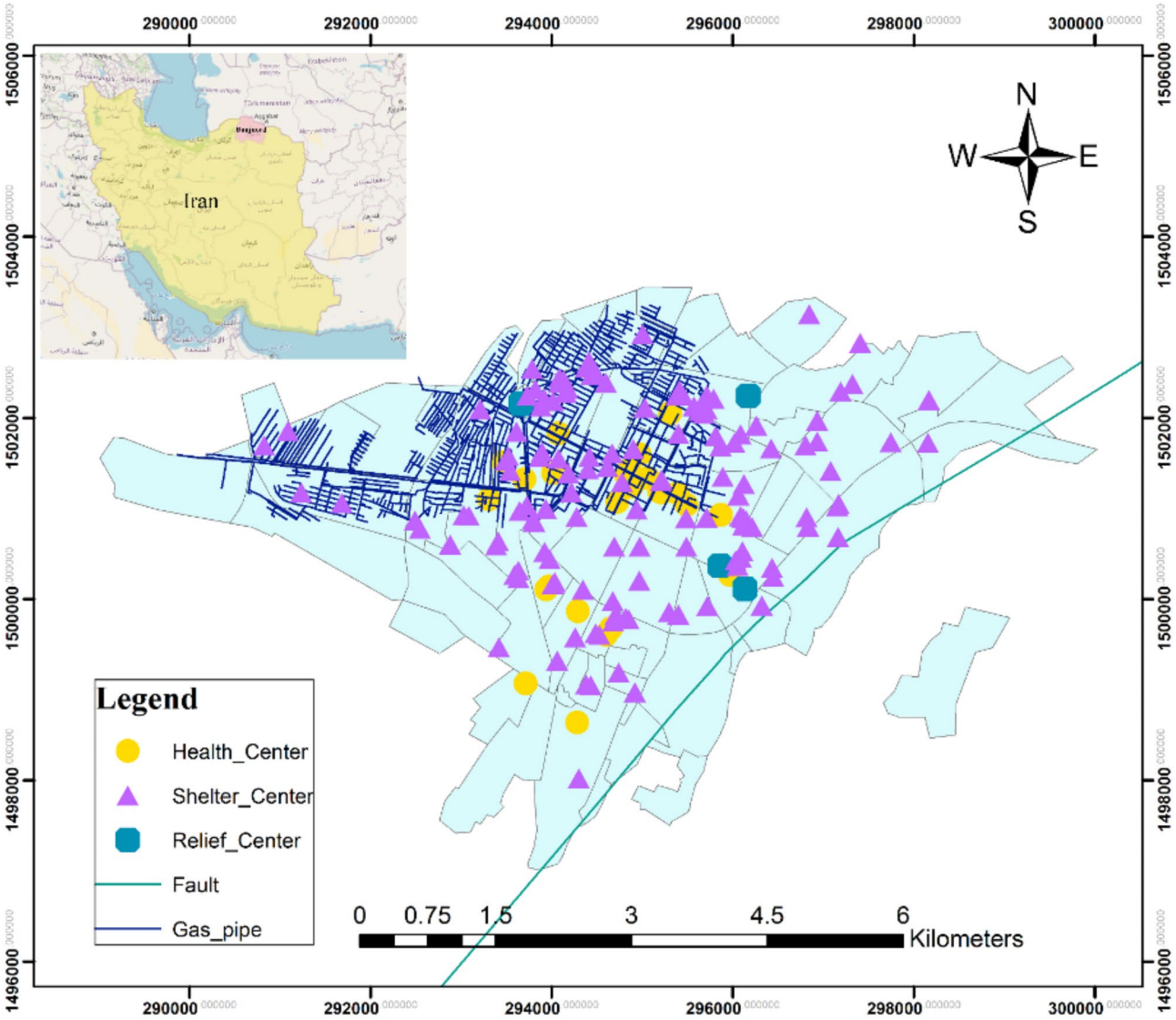

Fig. 2. The study area of Bojnord city, showing the locations of gas pipelines, faults, and health, relief, and shelter centers (Map generated using ArcGIS 10.5).

Gas pipeline data
Gas pipeline information was provided by the North Khorasan Gas Transmission Company for 2015. It includes specifications such as pipeline material (e.g., steel, cast iron, plastic), internal gas pressure levels, diameters, and lengths. This information is critical for identifying and analyzing hazards associated with gas infrastructure.

Population data
Population data were sourced from the Statistics Center of Iran, based on the latest national census conducted in 2016. This tabular dataset provides details on population size and age group distributions across residential districts and neighborhoods, which are essential for understanding demographic vulnerabilities.

Taxi origin-destination data
The taxi origin-destination dataset was collected between November 1 and December 26, 2018, from 137 taxis operating in Bojnord. The data were obtained via the Hamsi application, an online taxi booking platform managed by SACO Company. This dataset contains over 20 million records, including information on passenger pick-up and drop-off points, taxi ID, GPS coordinates, speed, time, travel direction, and passenger status (occupied or vacant). Temporal and spatial accuracy were ensured through 20-second time intervals and 5-meter spatial intervals, respectively.

To ensure the reliability and validity of the datasets, preprocessing steps were implemented to address inconsistencies and fill any missing information. Spatial datasets, such as land use and gas pipeline data, were processed using GIS tools to standardize formats and correct geospatial inaccuracies. Temporal datasets, such as taxi data, were aggregated and cleaned to address missing values and outliers. Gaps in categorical data, such as pipeline materials or demographic details, were addressed through interpolation or supplementary information from related studies.

Methodology

Spatial-temporal modeling is a powerful analytical tool that considers both geographical and temporal dimensions, providing a nuanced understanding of how phenomena evolve over time and space. In the context of urban resilience and risk assessment, incorporating spatial-temporal dynamics is crucial, as urban environments are inherently dynamic and subject to constant changes influenced by factors such as population movements, daily activities, and external events. This study adopts a two-fold approach: (a) assessing urban resilience against earthquakes, and (b) calculating earthquake risk. Each component is elaborated further in the subsequent subsections.

Spatial-temporal resilience assessment

The first part of the methodology focuses on evaluating the resilience of the city against earthquakes. Initially, the extraction and identification of criteria for the physical and social dimensions of resilience are conducted through library and documentary studies, previous research studies, the opinions of experts, field studies, and the availability of data. The information related to the two socio-physical dimensions is collected and extracted in the form of 27 components. Additionally, the method of collecting data is based on library and documentary research. By identifying the criteria, the information layers are prepared, and the criteria are standardized to be comparable using fuzzy functions. Then, the criteria are weighted with the DANP method and combined with the index overlay (IO) and ordered weighted averaging (OWA) methods. By combining the layers, the resilience of the city against earthquakes is determined. Due to the unavailability of gas pipeline information for the entire city of Bojnord, resilient spatial-temporal modeling is conducted for parts of Regions 1 and 2 of Bojnord city. Figure 3 shows the general steps in conducting the research, which are explained further.

Preparation of research criteria
In resilience studies, criteria selection involves two approaches: (1) a systematic review of the existing literature, ensuring compatibility with resilience concepts, and (2) the utilization of qualitative data from available sources. For this research, criteria for modeling the earthquake resilience of Bojnord city are developed based on the characteristics of the studied area. The criteria employed in this study are detailed in Table 2. In subsequent sections, the data and methodology used for generating population density criteria maps during the day, evening, and night, assessing the hazard of gas lines, and determining accessibility to vital centers are further explained.

Modeling the spatial-temporal population density In this research, spatial-temporal population modeling begins with data pre-processing. The first step in this study's data pre-processing involves extracting locations for passenger pick-up and drop-off to enable spatial-temporal population modeling. Such locations are identified by observing changes in passenger status. A passenger pick-up location is identified when there is a change from a passenger status of 0 to 1, whereas a drop-off location is identified when the passenger status changes from 1 to 0 (Fig. 4). Once the pick-up and drop-off locations are identified, points located outside the study area are removed. Subsequently, the number of trips generated and absorbed in each region is calculated.

Finally, spatial-temporal population modeling is performed using the obtained equations. In this study, the population during the day is determined using Eq. (1). Additionally, the number of people entering and leaving the study area is calculated using Eq. (2) and Eq. (3). To arrive at these values, several factors are considered, such as the statistical population of the region (CP), the population of the area during the day (P), and the population entering the region (P_d). The latter is calculated based on the number of passenger drop-off points (NDO), which represent absorbed trips. P_p refers to the exit population from the area, which can be calculated by the number of passenger pick-up points in the area (trips generated), i.e., NPU. α is the proportion of trips made by taxi.

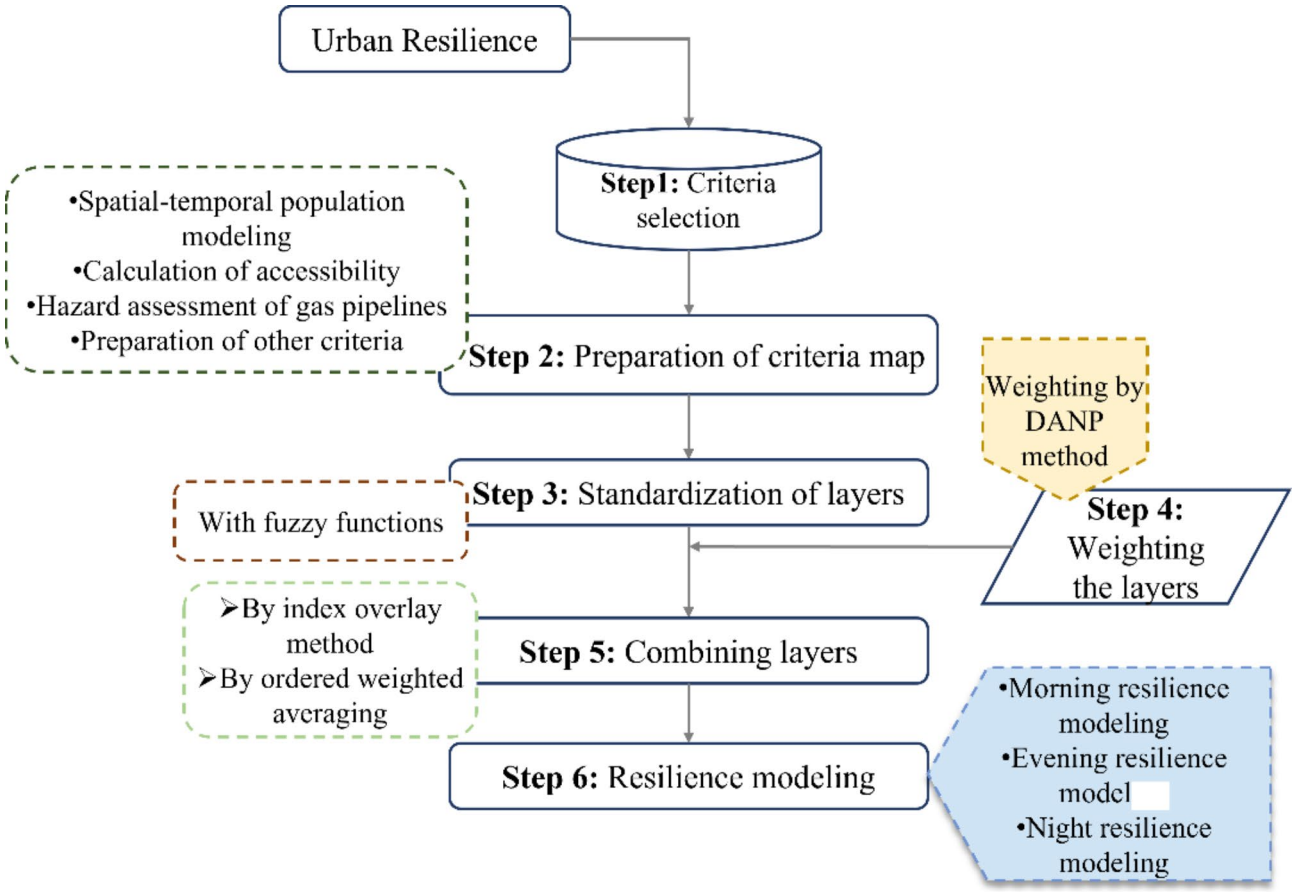

Fig. 3. General steps of research.

The value of α in this research is found to be 18.08%. In this research, morning, evening, and night population periods are considered. Figure 5 shows the steps of population spatial-temporal modeling[19].

$$P = CP + P_d - P_p \tag{1}$$

$$P_d = \frac{NDO}{\alpha} \tag{2}$$

$$P_p = \frac{NPU}{\alpha} \tag{3}$$

Assessing the hazard of gas pipelines in urban area To calculate the hazard of gas pipelines caused by the occurrence of an accident involving urban gas lines, the first step involves calculating the rate of gas release from the failure site using Eqs. (4) and (5)[20].

$$Q = C_0 A P_1 \sqrt{\frac{KM}{RT}\left(\frac{2}{K+1}\right)^{\frac{K+1}{K-1}}} \tag{4}$$

$$\mathrm{Q} = \mathrm{C_0 A P_1}\sqrt{\frac{2\mathrm{M}}{\mathrm{RT}}\left(\frac{\mathrm{K}}{\mathrm{K}-1}\right)\left[\left(\frac{\mathrm{P_0}}{\mathrm{P_1}}\right)^{\frac{2}{\mathrm{k}}} - \left(\frac{\mathrm{P_0}}{\mathrm{P_1}}\right)^{\frac{\mathrm{k}+1}{\mathrm{k}}}\right]} \tag{5}$$

These equations take into account factors such as the mass flow rate (Q) (Kg/s), molecular weight of the gas (M) (Kg/mol), gap area on the pipe (A) (m2), gas constant (R) (8.314 j/molkg), adiabatic index (K), temperature of the gas inside the pipe in Kelvin (T), ambient pressure in pascals (P0), and pressure inside the pipe in pascals (P1). After a line failure, there are several potential consequences, such as the release of toxic gases, sudden fires, jet fires, pool fires, fireballs, and explosions. The consequences of the fireballs, jet fires, and explosions generated by line damage are studied in this research. The dangerous range of pipelines is determined by calculating the lethality radius at three lethality levels of 1%, 50%, and 99% using Eq. (6) to (9).

Standardization (fuzzy membership function)	Sub criteria	Criterion	
Linear (incremental)	Accessibility to healthcare centers	Accessibility to vital centers	Physical dimension
Linear (incremental)	Accessibility to temporary shelter centers		
Linear (incremental)	Accessibility to relief centers		
Linear (decreasing)	Hazard assessment of gas pipelines	Hazard assessment	
Linear (incremental)	Distance from the fuel station	Distance from human danger zone	
Linear (incremental)	Distance from the power station		
Linear (incremental)	Distance from the gas station		
Linear (incremental)	Distance from the city gas lines		
Linear (decreasing)	Distance from the transportation network	Traffic factor (property of communication network)	
Linear (incremental)	Width of the roads		
Linear (incremental)	Type of roads		
Linear (decreasing)	Slope	Substrate characteristics	
User defined	Geological formation		
Linear (decreasing)	Distance from the fault	Distance from geological factors	
User defined	Type of material	Physical characteristics of the building	
User defined	Quality of building		
Linear (decreasing)	Age of the building		
User defined	Building facade		
Linear (decreasing)	Number of floors		
Linear (decreasing)	Occupancy level of the building		
Linear (decreasing)	Building Density		
User defined	land use		
Linear (incremental)	Building area		
Linear (decreasing)	Population density		
Linear (decreasing)	Age structure of the population	Demographic composition	Social dimension
Linear (incremental)	Gender structure of the population		
Linear (incremental)	Education level in the region		

Table 2. Standardization functions of criteria and sub-criteria.

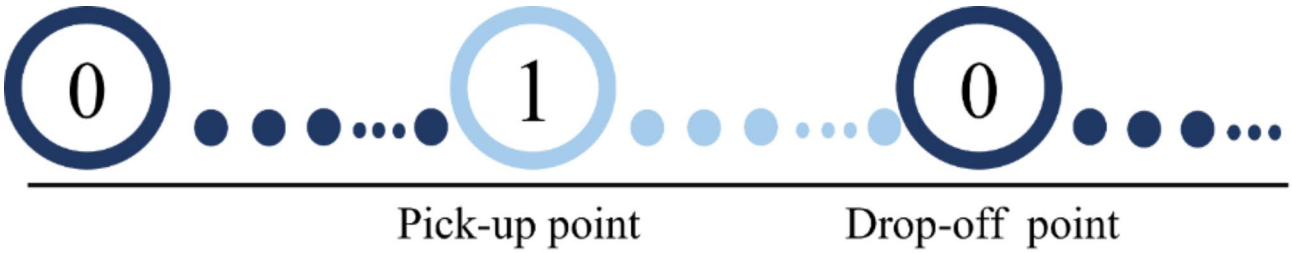

Fig. 4. Taxi data status.

$$r_{jet,99} = 3.891\sqrt{Q}, \quad r_{jet,50} = 5.498\sqrt{Q}, \quad r_{jet,1} = 7.767\sqrt{Q} \tag{6}$$

$$\frac{(r_{Fireball,99})^{\frac{4}{3}}}{m^{1.106}} = 2.855, \ \frac{(r_{Fireball,50})^{\frac{4}{3}}}{m^{1.106}} = 4.518, \ \frac{(r_{Fireball,1})^{\frac{4}{3}}}{m^{1.106}} = 7.149 \tag{7}$$

$$\frac{r_{Explosion,\,99}}{\sqrt[3]{m_{TNT}}} = 2.855, \ \frac{r_{Explosion,\,50}}{\sqrt[3]{m_{TNT}}} = 2.861, \ \frac{r_{Explosion,1}}{\sqrt[3]{m_{TNT}}} = 3.017 \tag{8}$$

$$m_{TNT} = \frac{m_d \Delta H_d}{Q_{TNT}} \tag{9}$$

$r_{jet,1}$, $r_{jet,50}$, and $r_{jet,99}$ represent the lethality radius of the eruption fire for three lethality levels of 99%, 50%, and 1%, respectively. $r_{Fireball}$ refers to the lethal radius for a fireball; m represents the mass of the gas; $r_{Explosion}$ refers to the lethal radius resulting from the explosion; and md represents the mass of the gas involved in the explosion. The length of lethality at three levels of 99%, 50%, and 1% for each grid point is calculated using Eq. (10). To determine the amount of hazard at each point, the pipes affecting the level of hazard created by the points are

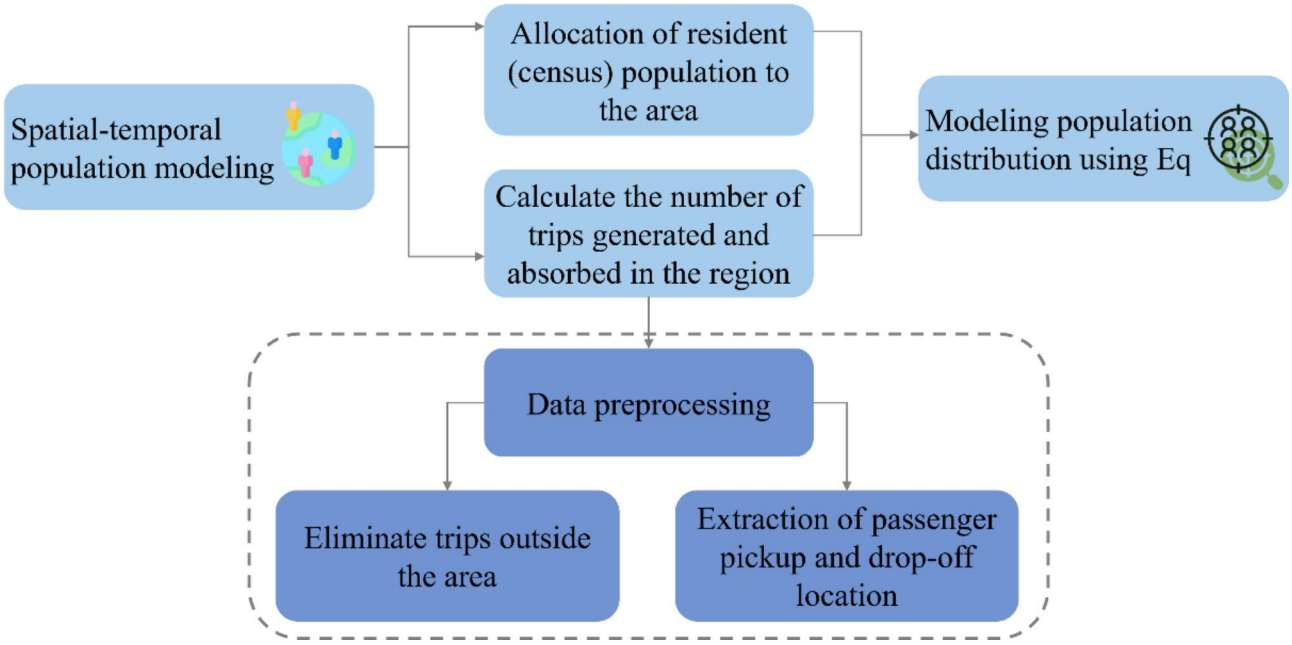

Fig. 5. Procedures for modeling population distribution.

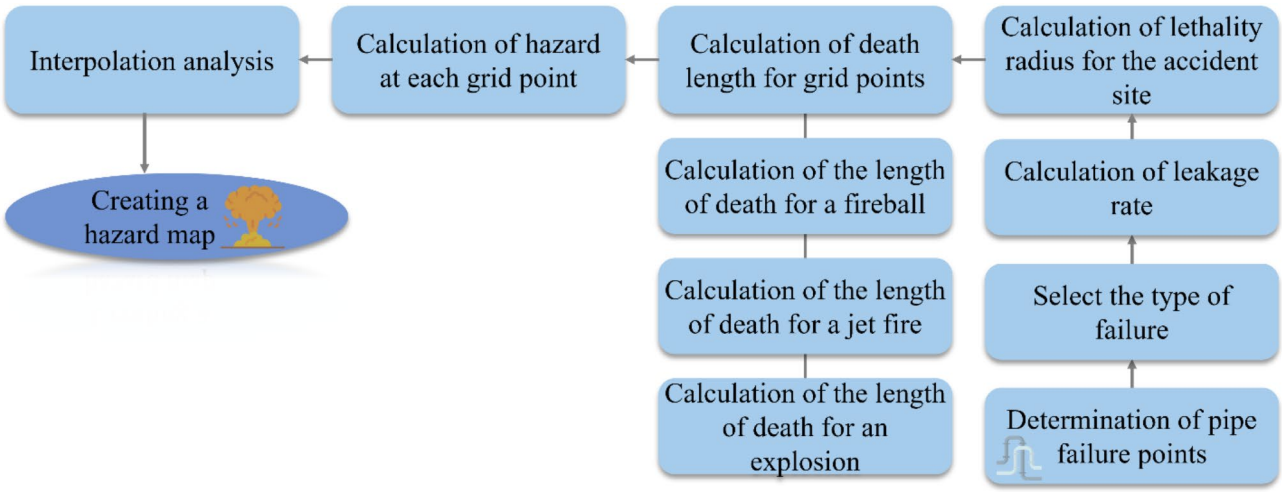

Fig. 6. Procedures for calculating gas pipelines hazards.

considered, and the lethality length is calculated for them. Finally, for each grid point, three values of the length of lethality caused by fireballs, jet fires, and explosions are obtained using Eq. (11) to (13). h represents the distance between the grid point and the location of the pipeline failure.

$$L_{i,100\_99} = 2\sqrt{r_{99}{}^2 - h^2}, L_{i,99\_50} = 2\sqrt{r_{99}{}^2 - h^2}, L_{i,50\_1} = 2\sqrt{r_{99}{}^2 - h^2} \tag{10}$$

$$L_{Fatal\ Length,\ jet\ fire} \approx l_{jet\ fire,\ 100\_99} + 0.805 l_{jet\ fire,99\_50} + 0.172 l_{jet\ fire,50\_1} \tag{11}$$

$$L_{Fatal\ Length,\ fireball} \approx l_{fireball,\ 100\_99} + 0.831 l_{fireball,99\_50} + 0.161 l_{fireball,50\_1} \tag{12}$$

$$L_{Fatal\ Length,\ explosion} \approx l_{explosion,\ 100\_99} + 0.828 l_{explosion,99\_50} + 0.168 l_{explosion,50\_1} \tag{13}$$

h is the distance between the grid point and the location of the pipeline failure. After calculating the mortality rate for the grid points of the study area, the hazard value is calculated using the product of the failure rate and the length of lethality at each grid point. After determining the hazard level for the grid points, the hazard level is calculated for the entire area using the interpolation tool. Failure rates for gas pipelines are determined using the EGIG database. Figure 6 shows the steps to calculate the hazard of gas pipelines[20].

Accessibility to critical centers In this research, to calculate accessibility to healthcare centers, relief centers (fire departments), and temporary sheltering centers, the two-step floating catchment area (2SFCA) method is employed. It is a special type of gravity model consisting of two stages. In the first step, the ratio of supply to demand is calculated. In this process, a circle centered on the center of gravity is drawn, and the amount of service provided to each neighborhood is determined. The first stage of the floating catchment area (supply-to-demand ratio) is calculated according to Eq. (14).

$$R_i = \frac{S_i}{\sum_{k \in \{d_{ik} < d_0\}} P_k} \tag{14}$$

where R_i is the ratio of healthcare, relief, and temporary shelter centers to the population at point j. S_i is the size of the healthcare, relief, and temporary shelter centers i. P_k represents the population of neighborhood k, whose center of gravity is covered by a buffer of 1.5, 1.7, and 0.9 km of healthcare, relief, and temporary shelter centers j ($d_{ik} \leq 1.5, 1.7, 0.9$ km). d_{ik} is the distance between k and i. In this research, the inverse function of distance is used to calculate accessibility. Therefore, the accessibility function is given in Eq. (15).

$$R_i = \frac{S_i}{\sum_{k \in \{d_{ik} < d_0\}} P_k d_{ij}^{\alpha}} \tag{15}$$

The second step calculates the availability of all healthcare, relief, and temporary shelter centers (A_{Center}) by summing all the R_i located in the buffer of each demand point. Equation (16) represents the second stage, showing the accessibility of centers for city neighborhoods[21,22].

$$A_{Center} = \sum_{i \in \{d_{ik} \leq 1.5,\ 1.7, 0.9\ km\}} R_i = \sum_{i \in \{d_{ik} \leq 1.5,\ 1.7, 0.9\ km\}} \frac{S_i}{\sum_{k \in \{d_{ik} \leq 1.5,\ 1.7, 0.9\ km\}} P_k} \tag{16}$$

where A_{Center} represents the accessibility for each neighborhood. Figure 7 shows the steps of accessibility calculation.

Standardization of layers

To integrate diverse criteria in resilience assessment, standardization is essential. This process converts various data types into a comparable scale, enabling meaningful evaluation. Fuzzy logic is employed for this purpose due to its flexibility in modeling complex relationships. It assigns values between 0 and 1 based on predefined membership functions, reflecting the degree of suitability or risk for each criterion[23]. In this study, linear fuzzy functions—including decreasing, increasing, and user-defined—are employed to transform criteria into fuzzy and standardized maps for further integration and assessment.

- *Increasing linear functions*: are used for criteria where higher values represent more favorable conditions for resilience. For instance, accessibility to healthcare centers is modeled using an increasing linear function because greater proximity enhances resilience.
- *Decreasing linear functions*: are applied to criteria where higher values indicate less favorable conditions. For example, the slope is modeled with a decreasing linear function, as steeper slopes contribute to higher vulnerability.
- *User-defined functions*: are utilized for criteria with non-linear relationships or for those requiring synthesis of multiple factors. For example, geological formation and building material types exhibit complex impacts on resilience, necessitating customized functions to accurately represent their influence.

This method ensures that all criteria, regardless of their original units or scales, are standardized for integration. Table 2 summarizes the functions applied to each criterion.

Weighting the layers

The process of weighting, or determining the relative importance of information, is conducted prior to the information integration operation. In this research, the Deterministic Analytic Network Process (DANP) method is employed for the weighting of information layers. The DANP method, introduced by Yang et al. in

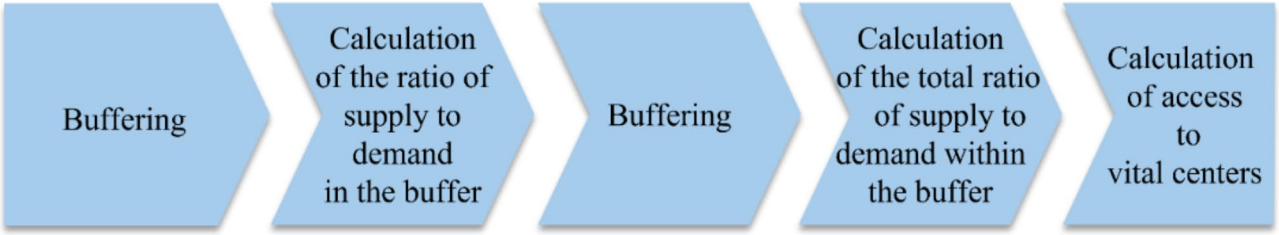

Fig. 7. Accessibility calculation steps.

2008, is a fusion of the Decision-Making Trial and Evaluation Laboratory (DEMATEL) and Analytic Network Process (ANP) methods. It is particularly suited for addressing problems with feedback or dependent criteria. The steps of the DANP process are detailed below:

Constructing the DEMATEL total correlation (TC) matrix The DEMATEL approach begins with an initial direct-relation matrix A, where each element a_{ij} represents the direct influence of criterion i on criterion j, as provided by expert judgments. The normalized direct-relation matrix D is calculated as Eq. (17)[24,25].

$$D = \frac{A}{max_{1 \le i \le n} \sum_{j=1}^{n} a_{ij}} \tag{17}$$

From D, the total correlation matrix T is computed (Eq. (18)).

$$T = D(I - D)^{-1} \tag{18}$$

Here, I is the identity matrix, and T captures both direct and indirect influences among criteria.

Identifying cause and effect relationships From the total correlation matrix T, the sum of rows (R_i) and columns (C_j) for each criterion are calculated (Eq. (19)).

$$R_i = \sum_{j=1}^{n} t_{ij} \ , \ C_j = \sum_{i=1}^{n} t_{ij} \tag{19}$$

The difference ($R_i - C_j$) determines whether a criterion is a cause ($R_i - C_j > 0$) or an effect ($R_i - C_j < 0$), while the sum ($R_i + C_j$) reflects the importance of the criterion.

Forming the ANP super matrix The normalized influence weights derived from DEMATEL are used to structure the ANP super matrix W, which integrates the interdependencies among criteria. The super matrix is then weighted and normalized to form a stochastic matrix.

Calculating final weights The final weights W_i of the criteria are derived by raising the weighted super matrix to a sufficiently large power until it converges to a steady-state distribution (Eq. 20). The resulting steady-state weights represent the relative importance of each criterion.

$$W^{\infty} = \lim_{k \to \infty} W^{k} \tag{20}$$

To obtain the necessary input for this weighting process, a detailed questionnaire is developed and distributed among seven experts, including five from crisis management departments and two academic professionals. Experts provide pairwise comparisons of the criteria, which form the input for the DEMATEL analysis. Consistency in expert opinions is verified using the Consistency Ratio (CR), calculated as Eq. (21):

$$CR = \frac{CI}{RI} \tag{21}$$

CI is the Consistency Index and RI is the Random Consistency Index. Only responses meeting the acceptable threshold for consistency ($CR \le 0.1$) are included in the analysis. Final weights are computed by averaging the experts' inputs, ensuring that individual biases do not disproportionately affect the results. The aim is to collect their opinions on the relative importance of factors that impact urban resilience against earthquakes, including hazard, vulnerability, and response capacity. The weights for the criteria and sub-criteria are determined using their responses to ensure a thorough and well-informed weighting procedure.

Combining criteria

After determining the weights for the 27 research criteria, the next step involves combining these criteria to assess the overall resilience. Each criterion carries varying degrees of importance, and the integration method plays a crucial role in shaping the resilience outcome. In this research, two methods, IO and OWA, are employed for this purpose.

The OWA model considers both the importance of weight and rank weight, offering a flexible approach to control the level of risk. This model provides a spectrum of potential solutions for resilience, accounting for deviation and dispersion of rank weights[26]. To implement the OWA model, the initial weight of the criteria is determined using the DANP method. The obtained weight is then multiplied by the rank weight of each criterion, and the sum is divided by the total number of criteria. In contrast, the index overlay method enables the combination of multiple maps, assigning weights to each layer based on the DANP method. The direct relationships between various system sectors or components are the main focus of the IO approach. The usual method for determining the impact of one factor on another is to utilize fixed weights that are based on actual data. The result classifies the studied area in terms of resilience[27]. Notably, the OWA method differs from the index overlay method by allowing the exchange of weights, facilitating control over risk-taking and risk aversion. In this research, the average operator is employed, balancing these considerations for practical urban planning applications. Combining these two approaches yields a strong framework that encompasses both the certainty of

present data and the uncertainty of future dangers, providing a thorough approach to resilience assessment. IO is chosen for its direct, data-driven insights, while OWA is selected for its flexibility.

Spatial-temporal earthquake risk assessment

This study defines earthquake risk assessment to include the urban environment's response capacity in addition to hazards and vulnerabilities. This definition considers an area's capacity to respond and manage the effects of an earthquake, allowing for a more comprehensive evaluation of risk. The risk is expressed in the form of Eq. (17)[14].

$$Risk\ (R) = Hazard\ (H) * Vulnerability\ (V) * Response\ Capacity\ (RC)$$

Seismic events and the effects they may have are referred to as hazards (H). Vulnerability (V) measures how vulnerable the population and infrastructure are to damage. Response Capacity (RC) evaluates the city's ability to respond to an earthquake and handle its consequences. This approach ensures that areas with strong reaction capabilities are recognized for their ability to reduce potential damage, offering a more comprehensive perspective of earthquake risk. Figure 8 shows the process of spatial-temporal earthquake risk assessment.

Hazard factor assessment

Evaluating seismic hazards, including Peak Ground Acceleration (PGA), proximity to hazardous materials, and the possibility of secondary hazards like fire, represents the main focus of the hazard factor assessment. These factors are combined and weighted based on their respective relative relevance to determine the hazard. The DANP approach is used to determine weights, ensuring an accurate representation of the importance of each hazard. PGA, which measures the maximum ground acceleration anticipated during an earthquake; proximity to hazardous materials, which measures the risk posed by such materials; and fire hazard, which assesses the potential for fire outbreaks after an earthquake, are all factors considered for hazard.

Vulnerability factor assessment

The vulnerability factor assessment in this earthquake risk study focuses on analyzing the several physical and social factors that influence how vulnerable metropolitan areas are to earthquake damage[16]. A combination of

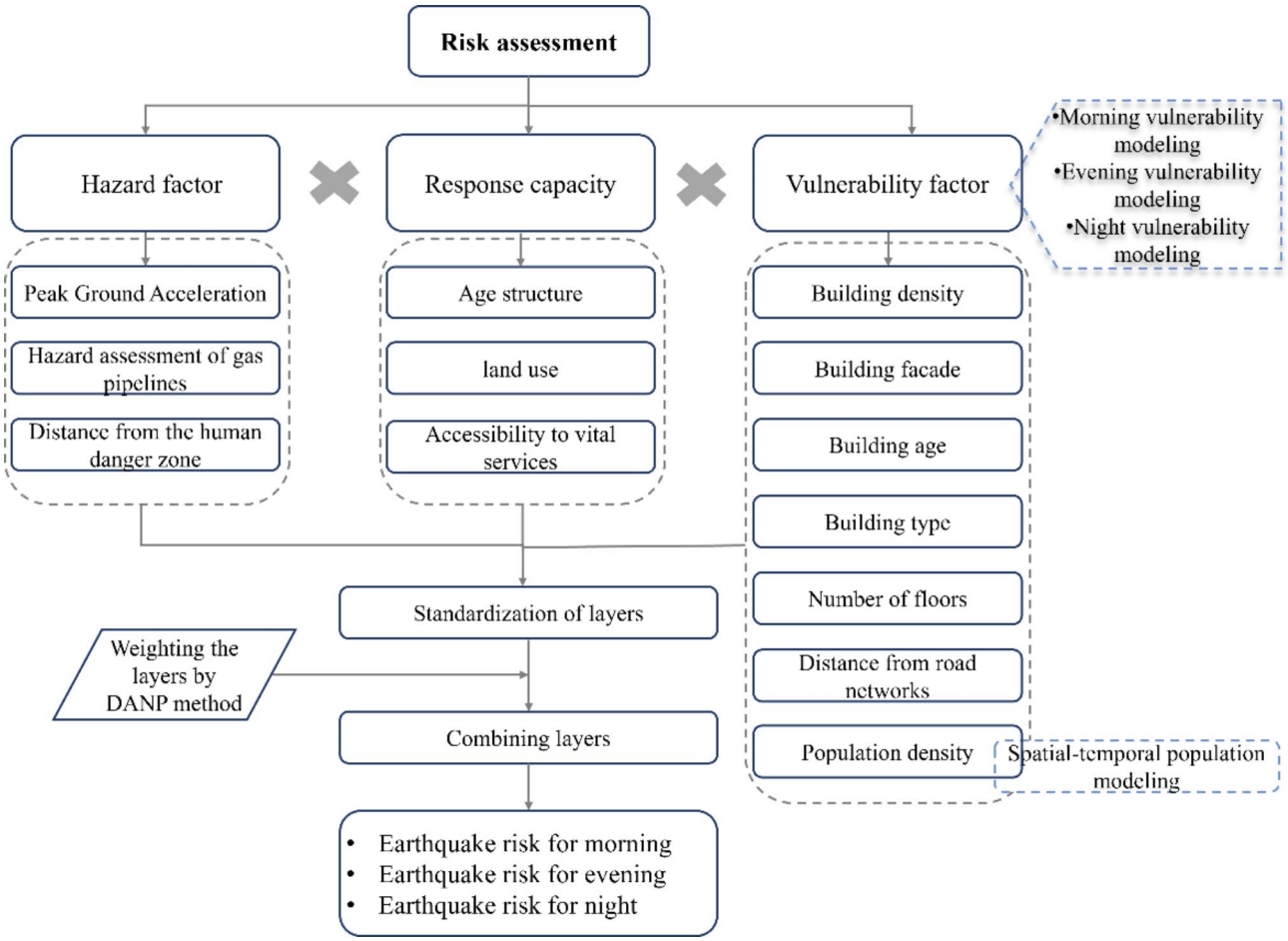

Fig. 8. Process of earthquake risk assessment.

built environment and population characteristics criteria is used to quantify the vulnerability factor. Each of these criteria is carefully chosen to reflect the possibility of damage and the influence on humans in the event of an earthquake. Building density, population density, building façade, building age, building type, number of floors, and distance from road networks are the criteria for assessing vulnerability. Each of these factors is assigned a weight according to its significance in contributing to the overall vulnerability of the area. Using a weighted sum technique, each of these factors is integrated into the overall vulnerability assessment. The weights are established by consulting experts and applying the DANP method. The result is a vulnerability score that provides a spatial representation of vulnerability across the study area.

Response capacity factor assessment

The primary objective of the response capacity evaluation in this earthquake risk assessment is to assess the city's capacity to efficiently handle and alleviate the consequences of an earthquake. The response capacity is quantified by analyzing several key factors that determine how well the city can respond to and recover from seismic events[15]. These criteria include the population's age distribution, land use in relation to open space access, and accessibility to vital services. These factors are evaluated to determine the RC score, and the DANP method is used to measure the weights allocated to each criterion. This score offers a thorough assessment of the city's readiness and capacity to handle the aftermath of an earthquake, highlighting areas with strong response capabilities and those in need of development. Finally, the risk assessment integrates the hazard, vulnerability, and response capacity indices into a single measure, providing an overall assessment of earthquake risk for each area.

Results

The results of the research are presented in this section, which is divided into three main subsections: the spatial-temporal resilience against earthquakes, the spatial-temporal earthquake risk assessment, and the integration of risk and resilience maps. Each subsection provides a detailed analysis of the various factors that contribute to the overall assessment of Bojnord City's vulnerability and preparedness for seismic events.

Spatial-temporal modeling of resilience

The aim of the present study was the spatio-temporal modeling of urban resilience against earthquakes. In this regard, 27 features related to the evaluation of urban resilience against earthquakes were considered. The standardized fuzzy map of all research indicators is presented in Fig. 9. According to the obtained fuzzy maps, the city of Bojnord was in a favorable situation in terms of social resilience, including the criteria of the education level of the region and the gender structure of the population. Furthermore, in terms of the physical dimension, the area level of the building, the distance from the transportation network, the slope, the geological formation, the age of the building, and the number of floors were in a favorable condition.

To model resilience, access criteria to critical centers were determined using the 2SFCA method and the hazard assessment of gas pipelines. Access to vital centers included access to healthcare centers, police centers, temporary shelters, and relief centers. In the calculation of access to vital centers, the results indicated that most areas had low access to service centers in the peripheral areas of the city, while the central areas of the city had better access to vital centers.

The purpose of the statistical and spatial analysis of the hazard of gas pipelines was to create a realistic picture of the probability of leakage, determine the effective factors, and create a network hazard assessment framework. In this section, an attempt was made to prepare a hazard map of gas pipelines for the three consequences of jet fire, fireballs, and explosions using the inherent parameters of gas pipelines and the surrounding environment.

In this study, a hazard map of urban gas pipelines was prepared by using the concepts of individual risk and calculating the amount of gas leakage, radius of lethality, length of death for grid points, and interpolation. Additionally, the effects caused by a fireball posed the greatest danger from natural gas leakage due to the large lethality radius. According to the gas pipe hazard map, the hazard level at the intersection of the main lines was higher due to the presence of connections and high gas pressure inside the pipe.

Imam Reza Hospital in the Mofkham neighborhood, Padegan Artesh, and Nirogah were population points during the day, while the residential areas of Koi Behadari, Nirogah, Mosala, and Koi Moalem at night were sensitive points on the hazard map. Therefore, by identifying high-danger areas, it was possible to reduce the probability of occurrence and the consequences of natural gas release accidents by taking safety measures, providing information about the loss of life and property, securing pipes, preventing leakage, and inspecting connections. The researchers utilized location-based data and taxi origin-destination information to model population distribution. The results showed that there were more taxi trips during the day than at night, and the daily population expanded from the city center to the suburbs due to urban development. The presence of various amenities, such as parks, stadiums, commercial centers, educational centers, and residential areas, contributed to high-density population centers.

The weighting results for resilience indicators are shown in Table 3, which highlights the substrate characteristics and physical characteristics of buildings as the most heavily weighted factors, while demographic characteristics have the least weight. With a weight of 0.131, the distance from the fault was the most important factor of the substrate. This suggested that during an earthquake, locations near fault lines were more vulnerable to strong ground shaking and potential damage. The hazard assessment of gas pipelines was another critical factor, with a weight of 0.114. Gas pipelines were a major source of risk during earthquakes because leaks could cause explosions and fires, which worsened the effects of the disaster[28]. Gas pipelines represented a systemic vulnerability that could lead to cascading failures across a city. For instance, a major gas pipeline rupture could result in extensive fires, explosions, and secondary damage that was significantly more severe than the effects of structural building failures alone[29]. These events were crucial to risk assessment because they hindered the

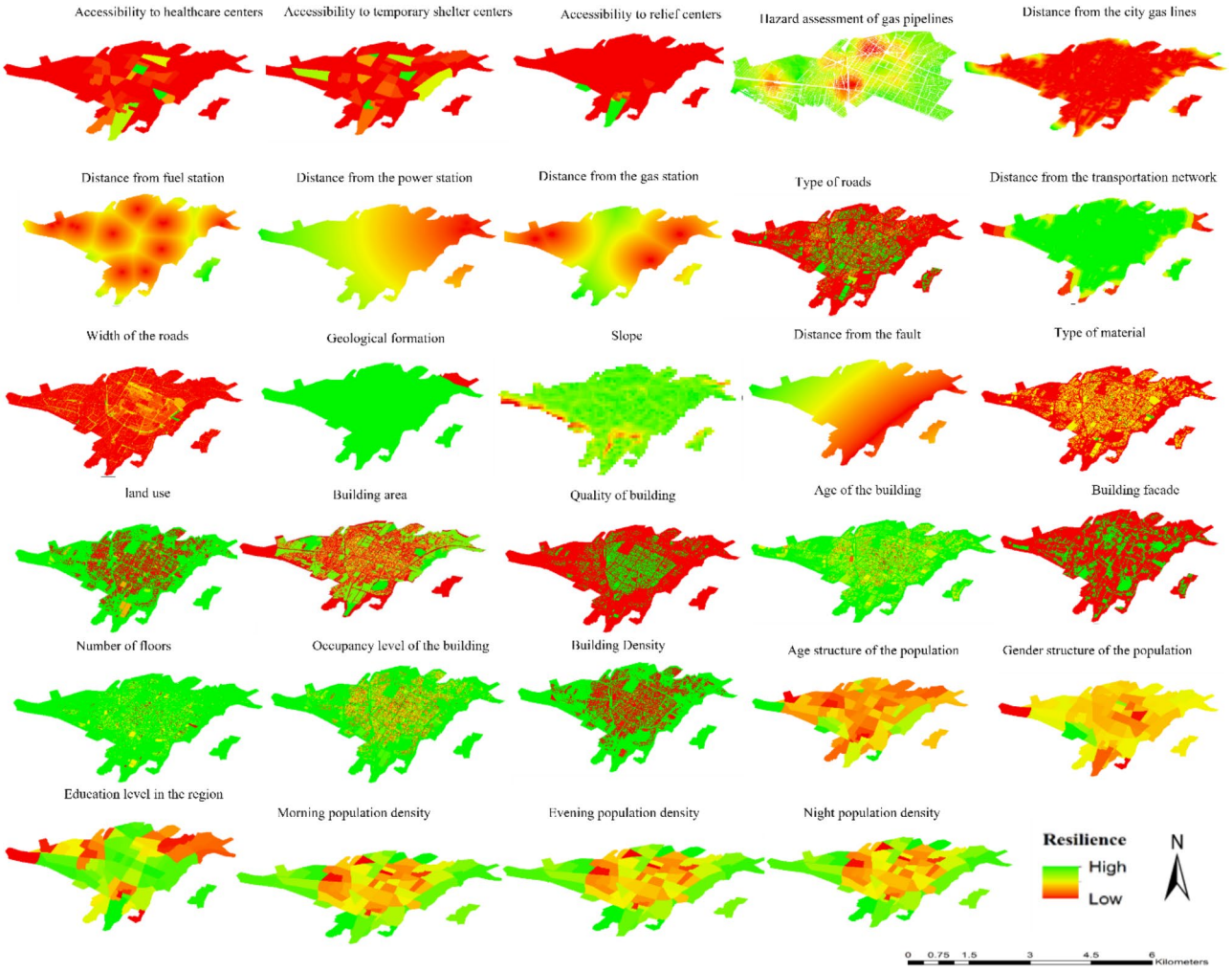

Fig. 9. Standardized layer of 27 research criteria (Map generated using ArcGIS 10.5).

efforts of emergency responders and increased overall damage. The third important consideration was the slope (0.0621) since steeper slopes raised the possibility of landslides, which could destroy infrastructure and make rescue efforts more difficult. The inclination or steepness of the land surface was referred to as the slope factor. Because steeper slopes were more likely to experience landslides during seismic events, which could seriously damage infrastructure and structures, this element was essential for resilience to earthquakes[30].

Among the traffic factors, the type of roads (0.0488) and road width (0.0477) emerged as highly significant. These factors were essential to ensuring that residents could evacuate effectively and that rescuers could reach impacted regions promptly. Access to temporary shelter centers (0.0461) was the most strongly weighted factor when it came to access to critical centers, highlighting the need for easily accessible shelters where people could take refuge immediately following a disaster. The weights assigned to access to healthcare centers (0.0435) and relief centers (0.0427) were comparable, highlighting the importance of immediate medical attention and assistance following an earthquake. Building density (0.0199) and population density (0.0185) were significant since they indicated the number of people and buildings that could be impacted. The region's education level, on the other hand, had the lowest weight (0.0066), suggesting that while it might not have had a direct influence on resilience immediately, it could have a major impact on recovery and preparedness efforts in the future.

Due to the lack of access to gas pipeline information for the entire city, the spatial-temporal map of the resilience of the city based on the IO and OWA methods was shown only for Region 1 and part of Region 2 of Bojnord city in Figs. 10 and 11. The terms "morning," "evening," and "night," as shown on these maps, indicated different scenarios according to the distribution of populations and different levels of human activity at various times of the day. Morning hours typically reflected peak commuting times, with a high concentration of activity in central business districts and transportation nodes. Evening hours captured the period when people were returning home, leading to activity dispersion towards residential areas. Nighttime hours represented periods of minimal activity, with most individuals located in their homes. These temporal divisions provided a comprehensive understanding of the shifts in resilience-related factors throughout the day. This method contributed to a better understanding of urban resilience by assessing how an earthquake's impact might have varied depending on the time of day.

Weight	Sub criteria	Weight	Criterion
0.0435	Accessibility to healthcare centers	0.132226	Accessibility to vital centers
0.0461	Accessibility to temporary shelter centers		
0.0427	Accessibility to relief centers		
0.114	Hazard assessment of gas pipelines	0.114055	Hazard assessment
0.0339	Distance from fuel station	0.128239	Distance from human danger zone
0.0281	Distance from the power station		
0.0388	Distance from the gas station		
0.0272	Distance from the city gas lines		
0.0459	Distance from the transportation network	0.14737	Traffic factor (property of communication network)
0.0477	Width of the roads		
0.0488	Type of roads		
0.0621	Slope	0.130692	Substrate characteristics
0.0605	Geological formation		
0.131	Distance from the fault	0.131067	Distance from geological factors
0.0142	Type of material	0.154021	Physical characteristics of the building
0.0135	Quality of building		
0.0143	Age of the building		
0.0138	Building facade		
0.0154	Number of floors		
0.0144	Occupancy level of the building		
0.0199	Building Density		
0.0172	land use		
0.0128	Building area		
0.0185	Population density		
0.0119	Age structure of the population	0.06233	Demographic composition
0.0098	Gender structure of the population		
0.0066	Education level in the region		

Table 3. Weighting results.

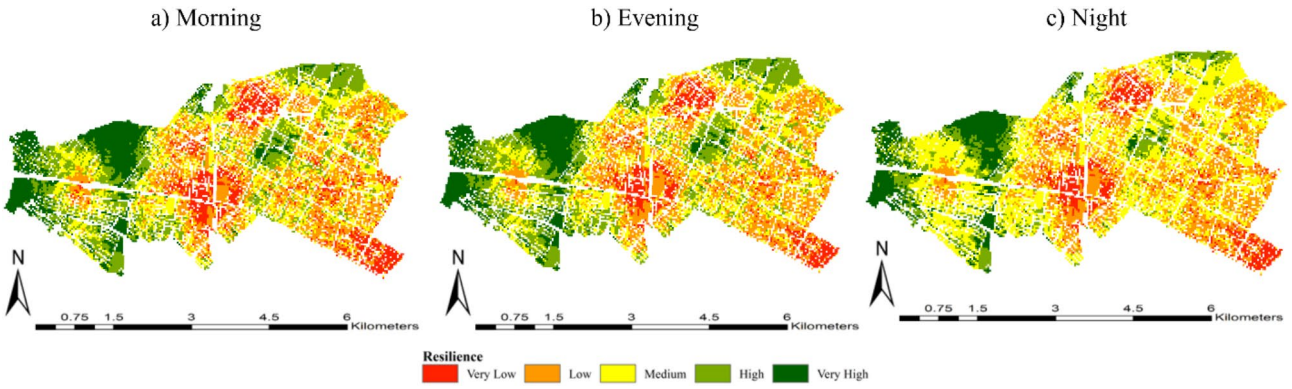

Fig. 10. Resilience map for Region 1 and part of Region 2 using IO method (Map generated using ArcGIS 10.5).

According to Figs. 10 and 11, most of the eastern part of Region 1 was in a disadvantageous situation and had less resilience, while some of the central parts of Region 1 exhibited low resilience. The western part of Region 1 demonstrated better resilience, with most of it having high to very high resilience. It is crucial to note that the morning and evening results, as illustrated in these maps, were notably consistent.

The percentage of the allocated area for the five classes of resilience—very high resilience to very low resilience—for morning, evening, and night in Region 1 and part of Region 2 based on the IO and OWA methods is shown in Figs. 12 and 13. According to Fig. 12, for the IO method, the very low resilience area constituted approximately 45.85% in the morning, decreased to 34.04% in the evening, and further reduced to 20.12% at night. This suggested that as the day progressed, there was a noticeable drop in highly vulnerable locations. The percentage of low resilience areas varied with the time of day: it was 31.37% in the morning, increased slightly

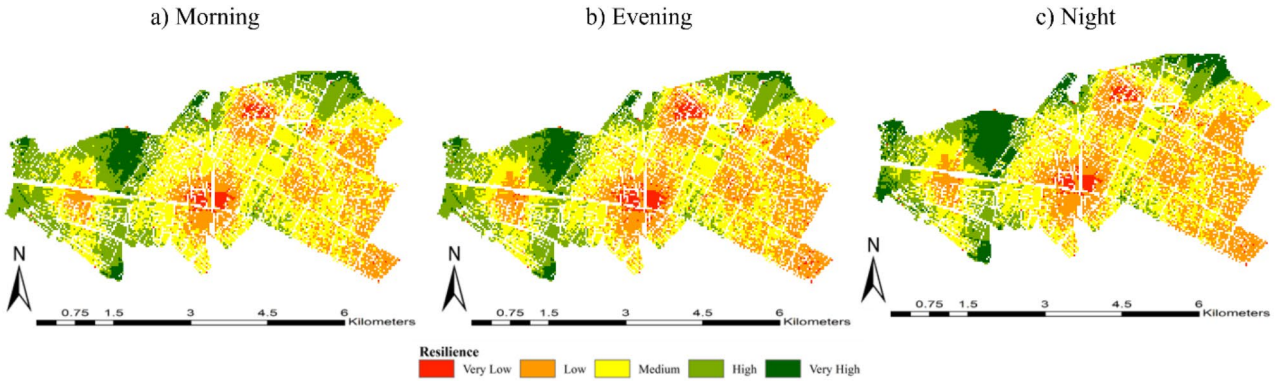

Fig. 11. Resilience map for Region 1 and part of Region 2 using OWA method (Map generated using ArcGIS 10.5).

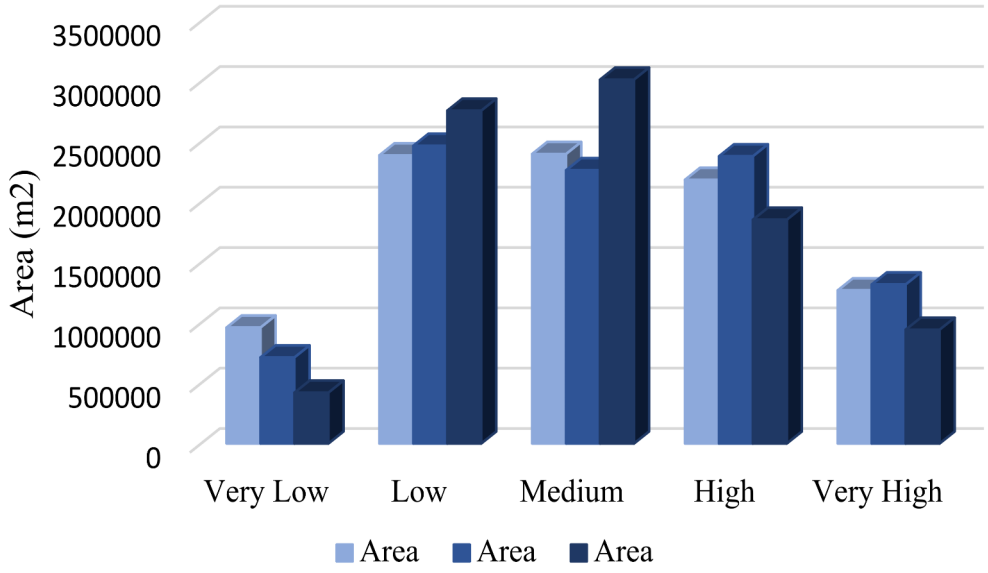

Fig. 12. Area affected by very high to very low resilience in three time periods using the IO method.

to 32.40% in the evening, and peaked at 36.23% at night. This suggested that low resilience zones were more noticeable at night.

The medium resilience category showed that medium resilience areas became more dominant at night. In the morning, they covered 31.25% of the area; in the evening, they dropped to 29.49%; and at night, they increased dramatically to 39.27%. High resilience areas constituted 34.04% in the morning, rose to 37.07% in the evening, and decreased to 28.88% at night, reflecting a shift in resilience as the day transitioned to night. Areas with very high resilience represented 35.95% in the morning, increased slightly to 37.33% in the evening, and decreased to 26.72% at night, suggesting that the highest resilience levels were most prominent during the evening.

According to the OWA method (Fig. 13), very low resilience covered 28.50% of the area in the morning, rose to 42.48% in the evening and then fell to 29.03% at night. This pattern suggested that there was a significant increase in vulnerability in the evening. Low resilience areas constituted 27.98% of the area in the morning, rose to 35.26% in the evening, and peaked at 36.76% at night. Nighttime was when low resilience zones were most noticeable. The morning period had the highest number of medium resilience areas, with medium resilience areas making up 35.91% of the total. These shares then declined to 32.14% in the evening and 31.95% at night. The area with high resilience started at 38.13% in the morning, decreased to 34.60% in the evening, and dropped further to 27.27% at night, indicating a reduction in high resilience areas as the day progressed. Very high resilience areas constituted 26.59% in the morning, remained almost steady at 26.55% in the evening, and surged to 46.86% at night. This significant increase at night suggested that certain areas exhibited enhanced resilience during this period, possibly due to reduced human activity or other factors.

Generally, both the IO and OWA methods followed a similar pattern across different times of day, reflecting consistent trends in resilience distribution. The distinctions between the two methods were not significant.

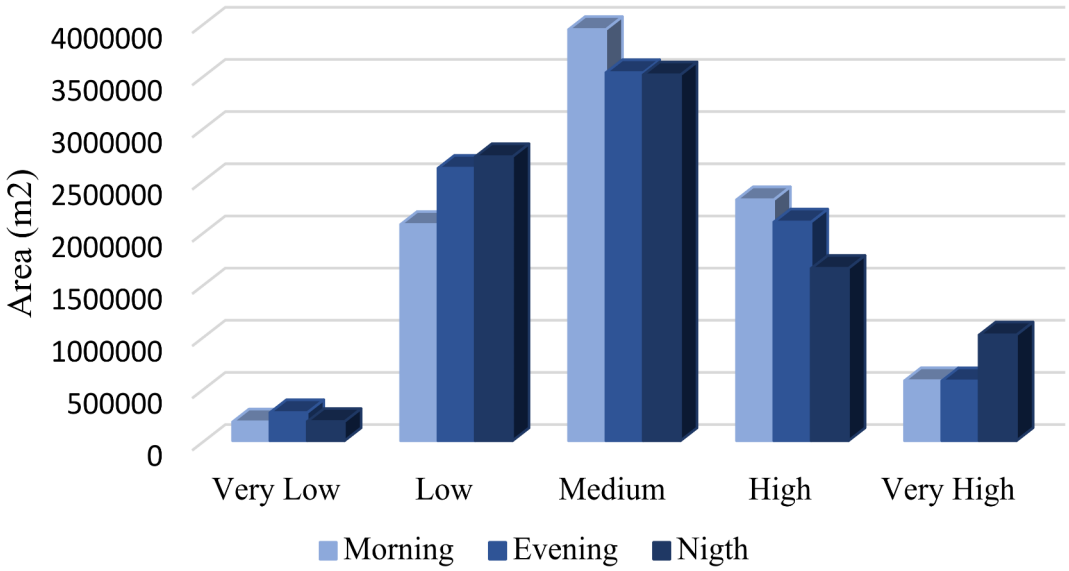

Fig. 13. Area affected by very high to very low resilience in three time periods using the OWA method.

These differences resulted from the different analytical approaches of the OWA and IO techniques. The IO method emphasized regularity over the day and offered a reliable and consistent assessment of resilience with a straightforward overlay technique. However, the OWA method offered a more dynamic and context-sensitive evaluation, resulting in more pronounced fluctuations in resilience levels, particularly during periods of changing human activity, such as the evening or night. This was because it incorporated a range of weights reflecting different levels of risk aversion or optimism.

Earthquake risk assessment

This subsection focuses on the spatial-temporal assessment of earthquake risk, integrating various factors that contribute to the likelihood and potential impact of seismic events. By combining hazard, vulnerability, and response capability criteria with a GIS-based methodology, we carried out an extensive earthquake risk assessment in this study.

Hazard assessment

The hazard assessment focused on variables affecting earthquake likelihood, assigning numerical weights to each variable based on its relative significance. PGA was identified as the most significant hazard factor, with a weight of 0.276, as it directly impacted the severity of ground shaking and potential structural damage. The hazard assessment of gas pipelines followed, with a weight of 0.208, due to the risk of leaks, explosions, and fires. Fuel stations were weighted at 0.145, reflecting the possibility of explosions or fires, while the distance from power stations was weighted at 0.141. Distance from gas stations and urban gas lines were both assigned weights of 0.115, highlighting their relevance in urban areas but indicating a lower comparative risk.

Figure 14 illustrates spatial variations in seismic hazard levels. The study area's center exhibited multiple zones classified as high hazard, attributed to the combined effects of high PGA, gas hazards, and proximity to fuel and power infrastructure. Surrounding areas showed high-to-medium hazard levels, particularly in the central and eastern regions, which represented broader areas of concern. In contrast, the western region showed low-to-very-low hazard levels, suggesting that it lay outside the primary danger zone for humans.

Spatial-temporal vulnerability assessment

The vulnerability assessment was based on structural and demographic factors, each weighted to reflect its contribution to overall risk. Building density and building age emerged as the most critical factors, each assigned a weight of 0.179, as they directly influenced the likelihood of damage and casualties in densely built and older structures. The building type and facade were given a weight of 0.134, reflecting their importance in assessing structural integrity and the likelihood of collapse during an earthquake. With a weight of 0.133, the number of floors in the buildings was also deemed significant because taller structures are typically more vulnerable. Population density received a weight of 0.13, given its importance in assessing the potential human impact. Finally, in recognition of the challenges in providing emergency response and evacuation in less accessible areas, the distance from road networks was weighted at 0.111.

Different patterns of vulnerability were observed throughout the study area, as revealed by the spatial-temporal vulnerability assessment (Fig. 15). The map illustrated varying levels of vulnerability, ranging from very low to very high. The western part of the area predominantly showed low to very low vulnerability. This could be attributed to factors such as a lower population and building density, fewer floors, newer buildings, and better access to transportation networks, all of which reduced seismic risk. In contrast, the central region presented a more mixed pattern. This region reflected a varied urban environment with a greater prevalence of

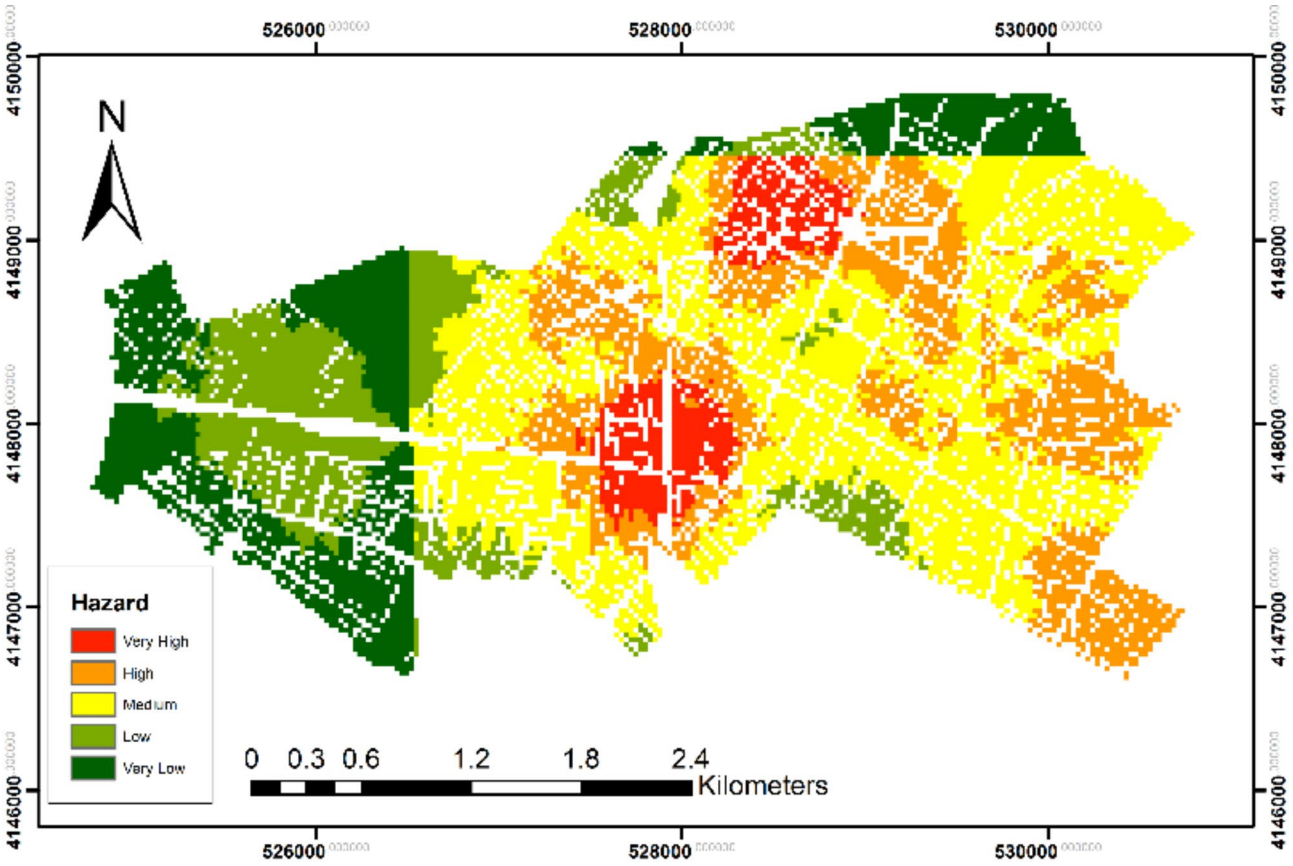

Fig. 14. Hazard map of the study area (Map generated using ArcGIS 10.5).

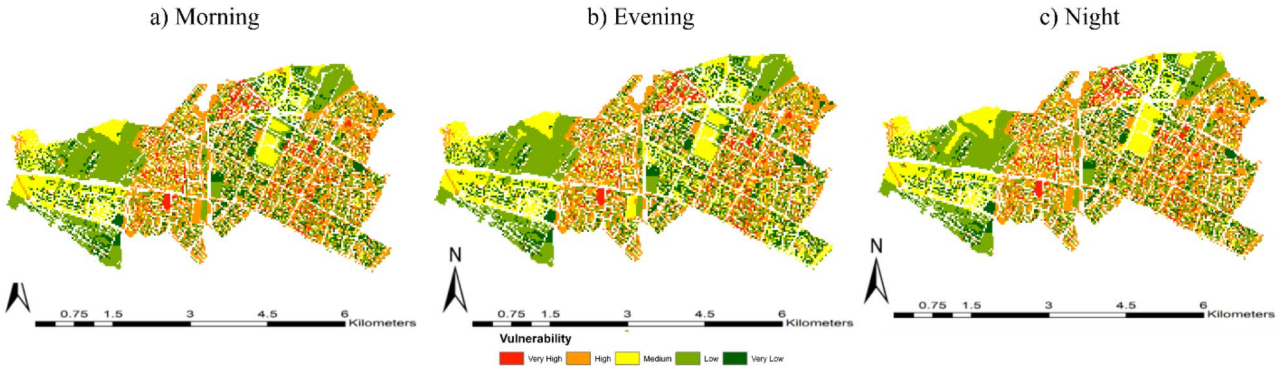

Fig. 15. Vulnerability map for study area (Map generated using ArcGIS 10.5).

older buildings, higher concentrations of population and structures, and less suitable building types, all of which contributed to moderate to high vulnerability. The eastern region was typically characterized by moderate to high vulnerability. This area was distinguished by a high concentration of structures and dense population, both of which increased the likelihood of damage during seismic events.

The evaluation also showed minimal temporal variations in vulnerability levels throughout the day. Notably, the vulnerability patterns in the morning and evening were quite similar, with only minor variations in spatial distribution. These temporal differences suggested that factors such as population density and activity levels could slightly influence vulnerability, but the overall patterns remained consistent.

Response capacity factor assessment

The evaluation of response capacity involved a weighted assessment of the accessibility of vital services and infrastructure. Land use played a major role, weighted at 0.231, especially in areas designated for emergency management and open spaces. Accessibility to healthcare centers was also heavily weighted at 0.224, reflecting

the critical need for timely medical care during a disaster. The accessibility of temporary shelters and relief centers was assigned a weight of 0.198, as these facilities played an essential role in providing immediate shelter and aid to displaced populations. Lastly, the age structure of the population was considered with a lower weight of 0.148, recognizing the challenges posed by aging populations during emergencies.

The spatial distribution of response capacity within the study area exhibited significant variability, as illustrated in Fig. 16. Very low response capacity was observed in the central part of the research area, highlighting potential weaknesses in accessibility to vital services and open land use. The dense urban fabric in this region was likely to put substantial stress on infrastructure during emergencies, reducing the effectiveness of disaster response efforts. The presence of an aging population further exacerbated these challenges, making the central area even less equipped to respond effectively to seismic events. On the other hand, the western parts of the study area typically showed high to very high response capacity. This could be attributed to open land use patterns and newer infrastructure, which enhanced emergency response operations. These regions demonstrated a greater potential for effective disaster relief and recovery from seismic events. The regional variations in response capacity underscored the need for targeted interventions in areas with low response capacity, particularly in central regions, to improve resilience against earthquakes.

Spatial-temporal risk mapping

The results of the hazard, vulnerability, and response capacity studies were integrated into the spatial-temporal earthquake risk assessment, visually represented in Fig. 17. This provided a comprehensive understanding of seismic risk across different regions and times of the day. The central region was consistently identified as a high-risk zone in all temporal scenarios due to a convergence of high seismic hazard, elevated vulnerability, and low response capacity. Risk levels increased during peak daytime hours, driven by increased population density caused by commercial activity, which highlighted the urgent need for focused risk mitigation strategies in this area.

The western part of the study area consistently exhibited lower earthquake risk due to a combination of lower seismic hazard, reduced vulnerability, and higher response capacity. This region benefited from newer buildings, better infrastructure, and less densely populated areas, all of which contributed to its resilience against seismic disturbances. While the overall risk distribution remained relatively stable throughout the day, subtle temporal variations were observed. Risk levels were slightly higher during the morning and evening scenarios, which corresponded to increased population movements and urban activity. In contrast, the late-night scenario reflected reduced risk due to lower population density and less strain on urban infrastructure. Although these temporal variations were not dramatic, they emphasized the importance of considering time-of-day factors in planning emergency preparedness and response strategies.

Fig. 16. The response capacity map in the study area (Map generated using ArcGIS 10.5).

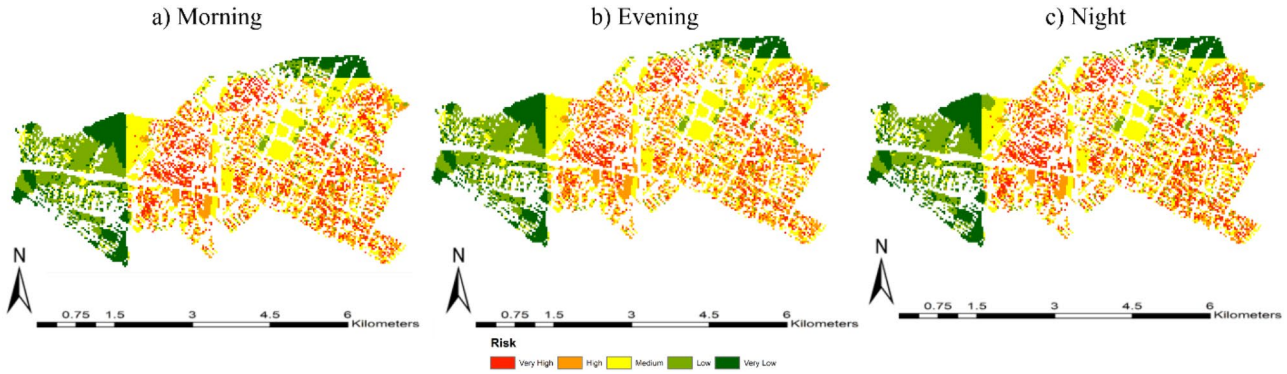

Fig. 17. Earthquake risk map of study area (Map generated using ArcGIS 10.5).

Discussion

The discussion below delves into the spatial-temporal dynamics of resilience, the integration of risk assessment and resilience, implications for urban planning and policy, and the limitations of the study.

Spatial-temporal variations in resilience and risk

Resilience varied significantly across Bojnord, with lower resilience observed in central, eastern, and northern areas due to factors such as high population density, older infrastructure, and socioeconomic challenges. Western and southern areas exhibited higher resilience, benefiting from modern infrastructure and lower population density, though localized risks persisted due to strategic assets or geological factors. These findings align with previous research on resilience in other Iranian cities[31–33].

Temporal variations in resilience were linked to population distribution patterns. Resilience was lower during peak hours (morning and evening) due to increased human activity and urban mobility, while nighttime exhibited higher resilience and lower risk. These insights underscore the need for disaster management strategies that account for both spatial and temporal dynamics.

Integration of risk assessment and resilience modeling

One critical insight derived from our approach was the identification of high-risk areas, which tended to coincide with high levels of vulnerability and hazard, coupled with low RC. These high-risk locations were especially vulnerable to the negative consequences of earthquakes; they were frequently characterized by older buildings, dense population densities, and socioeconomic difficulties. When these factors combined, they created significant limitations on the ability to respond effectively to disasters, leading to potentially catastrophic consequences. Building on the identification of consistently high-risk areas and those with temporal fluctuations in risk (morning, evening, night), the following interventions are designed to address both spatial and temporal vulnerabilities effectively:

For consistently high-risk areas

These areas remain vulnerable due to structural, socioeconomic, and environmental factors. Interventions should focus on long-term resilience building.

- *Strengthening Infrastructure*: Retrofit older buildings, reinforce critical lifeline systems such as gas pipelines, and upgrade urban infrastructure to reduce structural vulnerabilities.
- *Public Awareness and Preparedness Programs*: Implement continuous educational campaigns and regular earthquake drills to enhance community readiness across all time periods.
- *Advanced Monitoring Systems*: Deploy early-warning systems and real-time hazard-monitoring technologies to facilitate timely evacuation and response, regardless of the time of day.

For areas with temporal risk variations

Certain areas may experience heightened risk due to population density shifts at different times of the day. Adaptive, time-sensitive measures are essential.

- *Enhancing Emergency Service Accessibility*: Allocate flexible emergency resources, such as mobile healthcare units and temporary shelters, during peak risk periods. For example, increase emergency service coverage during busy morning commutes and in residential zones at night.
- *Smart Urban Planning*: Adjust urban development strategies by redistributing population density through incentives for housing in lower-risk areas and integrating green spaces that can serve as emergency shelters, considering both spatial and temporal risk dynamics.

Conversely, regions identified as having lower risk generally exhibited higher RC, reduced vulnerability, and lower hazard potential. These areas often benefited from newer infrastructure, better urban planning, and more robust emergency preparedness systems. The study found that in these regions, the capacity to withstand and

recover from disasters was significantly higher, resulting in a more resilient urban environment. However, the study also revealed that the relationship between resilience and risk was not always straightforward across the city. In some specific areas, resilience and risk did not follow an inverse relationship. For example, certain areas located on fault lines were considered high-risk, even though they had recently improved their infrastructure or implemented efficient emergency management systems, making them relatively resilient. These areas highlighted the complexity of urban resilience, where multiple factors intersected to influence the overall risk profile.

The findings further suggested that while areas with high resilience were generally better equipped to handle disasters, there were still pockets of vulnerability that could lead to disproportionate impacts. For instance, high-resilience areas might still contain vulnerable populations or critical infrastructure that, if damaged, could have cascading effects on the broader urban system. This underscored the necessity of a nuanced approach to resilience-building—one that addressed specific risks within high-resilience zones in addition to enhancing the general resilience of an area.

Enhancing earthquake resilience and risk: implications for urban planning and policy

To enhance earthquake resilience in Bojnord, or similar cities, urban planners and policymakers should focus on several critical steps based on the findings of this study. First, strengthening building codes and infrastructure is essential. Urban planners should ensure that all new constructions comply with updated seismic building codes that specifically address the vulnerabilities identified in the study, particularly in high-risk areas. Retrofitting older buildings, especially in densely populated and high-risk zones, should be prioritized to reduce potential damage during earthquakes. Additionally, critical infrastructure, such as hospitals, schools, and emergency response facilities, must be assessed and reinforced to ensure that they can withstand seismic events, which is crucial for maintaining essential services during a disaster.

A crucial next step is to implement focused interventions in high-risk locations. Zones with a high level of vulnerability, hazard, and poor response capabilities should be identified and given priority by policymakers for targeted disaster risk reduction initiatives. This may include creating community-based disaster response teams, designing emergency escape routes, and implementing targeted retrofitting initiatives to strengthen the resilience of the most at-risk populations. To improve disaster readiness through education, drills, and the distribution of emergency supplies, it is also essential to involve populations in high-risk areas.

Enhancing the control of spatial-temporal risks is an additional critical issue. Planners should put in place procedures that take into consideration the study's findings about temporal differences in risk, especially in the morning and evening when activity is at its highest. It is critical to optimize emergency response plans to increase their effectiveness during these high-risk periods. Improving responsiveness is also essential. Policymakers must ensure that emergency services, such as fire departments, healthcare facilities, and search-and-rescue teams, are suitably prepared and positioned to react promptly to seismic events, particularly in designated high-risk areas. Reducing casualties and damage requires implementing or upgrading early warning systems to instantly notify emergency services and the public.

Another crucial stage in urban planning is the integration of risk and resilience data. The study's resilience and risk maps should be incorporated into the city's urban planning framework. This will direct future zoning and development decisions to steer clear of high-risk locations and, where needed, increase resilience. Resilience and risk information must be incorporated into long-term urban planning strategies, including housing, public spaces, and transportation planning for every facet of urban development. Finally, it is critical to consistently review and adjust plans. The implementation of continuous monitoring systems for resilience and risk variables will facilitate the periodic reevaluation and modification of tactics in response to changes in urban dynamics. To ensure that resilience measures remain effective over time, policies and programs must be flexible and adaptive to new data, technological breakthroughs, and changing urban environments. Bojnord's resilience to earthquakes can be significantly enhanced by concentrating on these crucial measures, thereby lessening the possible effects of upcoming seismic events on the built environment and the population.

Limitations of the study

While this study offers a strong framework for evaluating risk and urban resilience, it is crucial to recognize several limitations that could compromise the precision and thoroughness of the results. The use of publicly accessible data, which is readily available but may not contain the most up-to-date or all relevant information, is a major drawback. For example, vital information about vulnerable groups, such as people with disabilities, was absent, which may have understated the need for resilience in some places.

Additionally, the study's focus on two specific regions within Bojnord may limit the generalizability of the results, making it challenging to apply the findings universally across different urban contexts. Another significant limitation lies in the inherent complexity of urban resilience, which is influenced by a multitude of dynamic factors. This study considered a select number of criteria, yet urban resilience is affected by many more variables, such as real-time traffic patterns, fluctuations in utility demand, and rapidly changing environmental conditions. For instance, the incorporation of real-time traffic data could significantly improve the assessment of evacuation routes and accessibility during emergencies by allowing for dynamic modeling of road congestion and route optimization. The study may overlook important temporal dynamics that could influence resilience by not including these factors, leading to an oversimplified analysis. Moreover, although the study focuses on population distribution at different times of the day—morning, evening, and night—demographic subgroup resilience (e.g., age structure, educational status, and gender) is only partially addressed. Resilience can vary significantly across different population groups[34], and further research should delve deeper into these aspects to provide more targeted insights.

Finally, while multi-criteria decision-making methods like DANP and the integration of criteria through the IO and OWA methods are powerful tools, they also introduce certain trade-offs. Including a broader range

of criteria can increase the comprehensiveness of the analysis but may dilute the precision and accuracy of the results due to the complexity of weighting and integrating diverse data sources. This balance between comprehensiveness and accuracy is a crucial consideration, as an overly complex model may introduce errors or uncertainties that could affect the reliability of the findings.

Conclusion and future work

The main goal of this research was to assess the earthquake resilience and risk of Bojnord City by developing a comprehensive structure that incorporates multiple criteria, such as the accessibility of vital services, the hazard potential from gas pipelines, and the distribution of the population during the day. The results emphasized the need to take into account various times of day when assessing urban resilience, highlighting notable regional differences throughout the study area. The study also underscored the importance of developing round-the-clock resilience strategies, as some locations remained vulnerable regardless of the time of day. Consistent resilience patterns observed in this study indicate that some regions require targeted disaster preparedness and response planning interventions. Risk and resilience were correlated, with high-risk areas typically exhibiting lower resilience, especially in the city center. This association highlights the importance of targeted efforts to improve resilience in high-risk areas.

This study provides a strong foundation for understanding and enhancing Bojnord's urban resilience, as well as a methodological approach that can be adapted and applied to other cities facing similar risks. Geospatial information systems play a valuable role in spatial-temporal population modeling by enabling advanced spatial analyses. Future studies could better prepare for and manage disasters by investigating resilience at shorter time intervals, such as hours or days of the week. Exploring metaheuristic methods, such as fuzzy and genetic algorithms, also offers advanced modeling techniques for a more detailed understanding of the variables influencing resilience. Further research into additional spatial-temporal criteria and advanced geospatial analysis methods may lead to the development of more accurate and effective disaster management strategies. Other dynamic urban factors, such as real-time traffic patterns, utility demand fluctuations, and environmental conditions, should also be incorporated, as they could significantly impact urban resilience.

Data availability

The datasets generated and/or analyzed during the current study are not publicly available due to ethical and legal considerations, as we don't have the right to share it and have made a commitment to the relevant organization. However, they are available from the first author via email at fatemehr937@gmail.com on reasonable request.

Received: 18 April 2024; Accepted: 27 February 2025
Published online: 10 March 2025

References

1. Lu, X. et al. Quantification of disaster resilience in civil engineering: A review. *J. Saf. Sci. Resil.* **1** (1), 19–30 (2020).
2. Kodag, S. et al. Earthquake and flood resilience through Spatial planning in the complex urban system. *Prog. Disaster Sci.* **14**, 100219 (2022).
3. O'Brien, K., Sygna, L. & Haugen, J. E. Vulnerable or resilient? A multi-scale assessment of climate impacts and vulnerability in Norway. *Clim. Change*. **64** (1–2), 193–225 (2004).
4. Zhang, X. et al. Resilience in urban, rural, and transitional communities: an empirical study in Guangdong, China. *Int. J. Disaster Risk Reduct.* **84**, 103396 (2023).
5. Qie, Z. & Rong, L. Spatial–temporal human exposure modeling based on land-use at a regional scale in China. *Saf. Sci.* **87**, 243–255 (2016).
6. Solomon, A. et al. Analyzing movement predictability using human attributes and behavioral patterns. *Comput. Environ. Urban Syst.* **87**, p101596 (2021).
7. Cutter, S. L. et al. A place-based model for Understanding community resilience to natural disasters. *Glob. Environ. Change*. **18** (4), 598–606 (2008).
8. Cutter, S. L., Ash, K. D. & Emrich, C. T. The geographies of community disaster resilience. *Glob. Environ. Change*. **29**, 65–77 (2014).
9. Joerin, J. et al. The adoption of a climate disaster resilience index in Chennai, India. *Disasters* **38** (3), 540–561 (2014).
10. Parizi, S. M., Taleai, M. & Sharifi, A. Integrated methods to determine urban physical resilience characteristics and their interactions. *Nat. Hazards*. **109** (1), 725–754 (2021).
11. Zhao, Y. et al. *Exploring Relationships of Urban Seismic Resilience Assessment Indicators With a Fuzzy Total Interpretive Structural Model Method* (Engineering, Construction and Architectural Management, 2022).
12. Liu, L. et al. The spatio-temporal dynamics of urban resilience in China's capital cities. *J. Clean. Prod.* **379**, 134400 (2022).
13. Zhai, C. et al. A novel urban seismic resilience assessment method considering the weighting of post-earthquake loss and recovery time. *Int. J. Disaster Risk Reduct.* **84**, 103453 (2023).
14. Mili, R. R., Hosseini, K. A. & Izadkhah, Y. O. Developing a holistic model for earthquake risk assessment and disaster management interventions in urban fabrics. *Int. J. Disaster Risk Reduct.* **27**, 355–365 (2018).
15. Kamranzad, F., Memarian, H. & Zare, M. Earthquake risk assessment for Tehran, Iran. *ISPRS Int. J. Geo Inf.* **9** (7), 430 (2020).
16. Jena, R. et al. Seismic hazard and risk assessment: a review of state-of-the-art traditional and GIS models. *Arab. J. Geosci.* **13** (2), 50 (2020).
17. Aydın, M. C. et al. Earthquake risk assessment using GIS-Based analytical hierarchy process (AHP): the case of Bitlis Province (Türkiye). *Int. J. Environ. Geoinform.* **11** (1), 1–9 (2024).
18. *Welcome to EarthquakeList.org!* Available from: https://earthquakelist.org/
19. Rahimi, F. et al. Modeling population Spatial-Temporal distribution using taxis origin and destination data. *Sustainability* **13** (7), 3727 (2021).
20. Ma, L., Cheng, L. & Li, M. Quantitative risk analysis of urban natural gas pipeline networks using geographical information systems. *J. Loss Prev. Process Ind.* **26** (6), 1183–1192 (2013).
21. Giannotti, M. et al. Inequalities in transit accessibility: contributions from a comparative study between global South and North metropolitan regions. *Cities* **109**, 103016 (2021).

22. Guo, Y., Chan, C. H. & Yip, P. S. *Spatial Variation in Accessibility of Libraries in Hong Kong*. Library & Information Science Research, 319–329. (2017).
23. Javari, M., Saghaei, M., Fadaei, F. & Jazi Analyzing the resilience of urban settlements using multiple-criteria decision-making (MCDM) models (case study: Malayer city). *Sustainable Environ.* **7** (1), 1889083 (2021).
24. Hsu, C. H., Wang, F. K., Tzeng, G. H. & Resources The best vendor selection for conducting the recycled material based on a hybrid MCDM model combining DANP with VIKOR. *Conserv. Recycl.* **66**, 95–111. (2012).
25. Jamali, A. et al. Urban resilience assessment using hybrid MCDM model based on DEMATEL-ANP method (DANP). *J. Indian Soc. Remote Sens.* **51** (4), 893–915 (2023).
26. Marzi, S. et al. Constructing a comprehensive disaster resilience index: the case of Italy. *PloS One*. **14** (9), e0221585 (2019).
27. Jahangiri, K. et al. Site selection criteria for temporary sheltering in urban environment. *Int. J. Disaster Resil. Built Environ.* **11** (1), 58–70 (2020).
28. Jabbari, M. et al. *Risk assessment of fire, explosion and release of toxic gas of Siri–Assalouyeh sour gas pipeline using fuzzy analytical hierarchy process*. *Heliyon*. **7**(8). (2021).
29. Rahimi, F. et al. Temporal dynamics of urban gas pipeline risks. *Sci. Rep.* **14** (1), 5509 (2024).
30. Micu, M., Micu, D. & Havenith, H. B. Earthquake-induced landslide hazard assessment in the Vrancea seismic region (Eastern Carpathians, Romania): constraints and perspectives. *Geomorphology* **427**, 108635 (2023).
31. Shahpari Sani, D. et al. An assessment of social resilience against natural hazards through Multi-Criteria decision making in geographical setting: A case study of Sarpol-e Zahab, Iran. *Sustainability* **14** (14), 8304 (2022).
32. Bastaminia, A. et al. Assessing the Capabilities of Resilience against Earthquake in the City of Yasuj, Iran. In *Earthquake Disasters.* Routledge, 42–62. (2021).
33. Sharifi, A., Roosta, M. & Javadpoor, M. Urban form resilience: A comparative analysis of traditional, semi-planned, and planned neighborhoods in Shiraz, Iran. *Urban Sci.* **5** (1), 18 (2021).
34. Santos, J. et al. Workforce/Population, economy, infrastructure, geography, hierarchy, and time (WEIGHT): reflections on the plural dimensions of disaster resilience. *Risk Anal.* **40** (1), 43–67 (2020).

Acknowledgements

This work was supported in part by the ITRC Support Program under Grant IITP-2023-RS-2022-00156354 and in part by the Metaverse Support Program to Nurture the Best Talents under Grant IITP-2023-RS-2023-00254529 funded by the Ministry of Science and ICT of Korea and the Institute of Information and Communications Technology Planning and Evaluation (IITP).

Author contributions

Fatema Rahimi: formal analysis, methodology, software, investigation, writing—original draft preparation, visualization. Abolghasem Sadeghi-Niaraki: Conceptualization, methodology, software, validation, investigation, writing—review and editing, supervision. Mostafa Ghodousi: data curation, formal analysis, methodology, investigation, validation, writing—original draft preparation, visualization. Soo-Mi Choi: resources, validation, writing—review and editing, project administration, funding acquisition. All authors have read and agreed to the published version of the manuscript.

Declarations

Competing interests

The authors declare no competing interests.

Additional information

Correspondence and requests for materials should be addressed to S.-M.C.

Reprints and permissions information is available at www.nature.com/reprints.

Publisher's note Springer Nature remains neutral with regard to jurisdictional claims in published maps and institutional affiliations.